

## UBA6 and NDFIP1 regulate the degradation of ferroportin

Lisa Traeger,<sup>1</sup> Steffen B. Wiegand,<sup>1</sup> Andrew J. Sauer,<sup>1</sup> Benjamin H.P. Corman,<sup>1</sup> Kathryn M. Peneyra,<sup>1</sup> Florian Wunderer,<sup>1,2</sup> Anna Fischbach,<sup>1</sup> Aranya Bagchi,<sup>1</sup> Rajeev Malhotra,<sup>3</sup> Warren M. Zapol<sup>1</sup> and Donald B. Bloch<sup>1,4</sup>

<sup>1</sup>Anesthesia Center for Critical Care Research of the Department of Anesthesia, Critical Care and Pain Medicine, Massachusetts General Hospital and Harvard Medical School, Boston, MA, USA; <sup>2</sup>Department of Anesthesiology, Intensive Care Medicine and Pain Therapy, University Hospital Frankfurt, Goethe University, Frankfurt, Germany; <sup>3</sup>Cardiovascular Research Center and the Cardiology Division of the Department of Medicine, Massachusetts General Hospital and Harvard Medical School, Boston, MA, USA and <sup>4</sup>Division of Rheumatology, Allergy and Immunology of the Department of Medicine, Massachusetts General Hospital and Harvard Medical School, Boston, MA, USA

©2022 Ferrata Storti Foundation. This is an open-access paper. doi:10.3324/haematol.2021.278530

Received: February 6, 2021.

Accepted: July 22, 2021.

Pre-published: July 29, 2021

Correspondence: DONALD B. BLOCH - dbloch@mgh.harvard.edu

LISA TRAEGER - email@lisatraeger.de

## Supplemental Material and Methods

### Methods

#### *siRNA screen*

The day before siRNA transfection, cells were seeded in 8-well tissue culture slides in full growth medium without antibiotics to obtain a confluence of 30-50% on the day of transfection. The siRNA-library *Human Ubiquitin Conjugation Subset 1* (siGENOME® SMART pool® siRNA library G005615 Lot11132, which contains a mixture of four different siRNAs targeting each gene), as well as additional individual siRNAs directed against specific components of the ubiquitin pathway, were obtained from Dharmacon (Lafayette, CO, USA) (Supplemental Table 1). siRNA was transfected into cells using Dharmafect transfection reagent 4 (Dharmacon) according to the manufacturer's instructions. Cells were transfected using a final concentration of 20nM siRNA. Twenty-four hours after transfection, cells were washed, incubated with EMEM with 0.1% FBS and expression of FPN-GFP was induced by the addition of doxycycline for 16-18h. The following day, BMP6 (10ng/ml) or hepcidin (4ng/ml) or vehicle alone was added, and the cells were incubated for an additional 18h. To prepare protein extracts for immunoblot, cells were seeded and transfected in 6-well plates.

#### *Immunofluorescence*

Cells were fixed with 2% PFA for 10 min and permeabilized with methanol containing 4',6-Diamidin-2-phenylindol (DAPI) (0.5µM) for 7 min. Cells were stained with an antibody directed against GFP (Roche 11814460001, 1:250) for one hour at RT, followed by Alexa-488 conjugated donkey-anti-mouse antibody (Jackson ImmunoResearch, Cat. No 715545150; 1:250) for one hour. Cells were visualized using a Nikon Eclipse 80i (Nikon Instruments, Melville, NY, USA) microscope and the program Retiga 2000R, QIMAGING (Surrey, BC, Canada).

### *Immunoblot analysis*

Cells were lysed in RIPA buffer supplemented with a protease and phosphatase inhibitor cocktail (Thermo Fisher Scientific). Plasma enriched membrane proteins were prepared from liver using the Mem-PER™ Cell lysate kit (Thermo Fisher Scientific). Samples were prepared in Laemmli buffer without reducing agent and incubated for 30 min at RT<sup>1</sup>. Proteins were separated by SDS-Page, transferred to PDVF membranes, and incubated with primary antibodies overnight. Immunoblots were incubated with fluorescent dye-labeled secondary antibodies and imaged using the LI-COR Odyssey detection system (LI-COR, Lincoln, NE, USA). All of the antibodies used in this study are listed in supplemental table 2.

### *Quantitative Real-Time PCR*

Total RNA was extracted using Trizol (Qiagen, Germantown, MD, USA) according to the manufacturer's instructions. Complementary DNA was synthesized using MultiScribe Reverse Transcriptase (Applied Biosystems, Foster City, CA, USA). Quantitative Real-Time PCR was performed on the Mastercycler Replex (Eppendorf, Hamburg, Germany) using TaqMan Fast Advanced Master Mix (Applied Biosystems). Target gene expression was normalized to levels of 18S ribosomal RNA and calculated using the relative C<sub>T</sub> method<sup>2</sup>. TaqMan probes that were used for qPCR are listed in supplemental table 3.

### *Hepcidin and Iron analysis*

Hepcidin levels were determined using the Hepcidin-25 HS Elisa Kit (DRG International, Inc.; Springfield, NJ, USA) according to the manufacturer's instructions. Serum iron levels were measured using the Iron-SL kit (Seksui Diagnostics, Lexington, MA, USA) according to the manufacturer's instructions.

## Material

**Supplemental Table 1. List of siRNAs directed against components of the ubiquitin pathway.**

Initial E2/E3 Screen	
Gene Symbol	Gene Accession
UBE2C	NM_181803
UBR5	NM_015902
UBE2K	NM_001111113
HECTD1	NM_015382
UBE2T	NM_014176
CDC34	NM_004359
C12orf51	NM_001109662
DCUN1D1	NM_020640
CUL2	NM_003591
HERC3	NM_014606
UBE2W	NM_018299
UBE2V2	NM_003350
DCUN1D5	NM_032299
HERC2	NM_004667
UBE2N	NM_003348
UBE2Z	NM_023079
UBE2L3	NM_003347
HERC5	NM_016323
UBE2NL	NM_001012989
DCUN1D3	NM_173475
BIRC6	NM_016252
UBE2J2	NM_194457
UBA7	NM_003335
HERC1	NM_003922
HACE1	NM_020771
CUL7	NM_014780
UBE2S	NM_014501
CUL3	NM_003590
HUWE1	NM_031407
CAND2	NM_012298
UBE2D3	NM_181893

HECT E3 Screen	
Gene Symbol	Gene Accession
SMURF1	NM_181349
ITCH	NM_031483
NEDD4	NM_006154
WWP1	NM_007013
SMURF2	NM_022739
NEDD4L	NM_015277
HECW2	NM_020760
HECW1	NM_015052
WWP2	NM_001270453

UBA5	NM_198329
UBE2M	NM_003969
UEVLD	NM_018314
UBE2F	NM_080678
DCUN1D2	NM_001014283
CUL1	NM_003592
UBE3B	NM_130466
UBE2A	NM_003336
UBE2E2	NM_152653
HECTD3	NM_024602
UBE2I	NM_003345
UBE2Q2	NM_173469
HERC6	NM_017912
UBE2O	NM_022066
UBE2V1	NM_001032288
UBE2R2	NM_017811
AKTIP	NM_022476
UBE2E1	NM_003341
UBE3C	NM_014671
TSG101	NM_006292
UBE2G2	NM_003343
UBA3	NM_003968
UBE2E3	NM_006357
UBE2D1	NM_003338
UBE3A	NM_000462
TRIP12	NM_004238
HECTD2	NM_173497
CUL4A	NM_003589
HERC4	NM_015601
UBE2B	NM_003337
UBE2U	NM_152489
TMEM189- UBE2V1	NM_003349
CAND1	NM_018448
KIAA0317	NM_001039479
UBE2D4	NM_015983
DCUN1D4	NM_015115
CUL4B	NM_001079872
UBE2L6	NM_004223

UBE2J1	NM_016021
UBE2QL1	XM_940609
UBE2Q1	NM_017582
UBE2G1	NM_003342
UBE2H	NM_182697
CUL5	NM_003478
ARIH1	NM_005744
UBE2D2	NM_003339
CACUL1	NM_153810
NDFIP1	NM_030571

**Supplemental Table 2. List of Antibodies**

Name	Company	Catalog No.	Dilution
Mouse-anti-GFP	Roche	1181446000	1:1000
Rabbit-anti-FPN	Novus	NBP1-21502	1:1000
Rabbit-anti-Ferritin H-chain	Santa-Cruz	sc25617	1:1000
Rabbit-anti pSMAD1/5/8	Maine Medical Center Research Institute	VI131	1:1000
Rabbit-anti GAPDH	Cell Signaling	D16H11	1:2500
Rabbit-anti-NDFIP1	Abcam	ab236892	1:1000

**Supplemental Table 3. List of qPCR TaqMan Probes**

Human S18 TaqMan gene expression assay	Hs99999901_s1
Human UBA1 TaqMan gene expression assay	Hs01031318_m1
Human UBA6 TaqMan gene expression assay	Hs00414964_m1
Human NDFIP1 TaqMan gene expression assay	Hs00228968_m1
Human ARIH1 TaqMan gene expression assay	Hs00194934_m1
Human HAMP TaqMan gene expression assay	Hs00221783_m1
Human ID1 TaqMan gene expression assay	Hs03676575_s1
Mouse S18 TaqMan gene expression assay	Mm03928990_g1
Mouse Ndfip1 TaqMan gene expression assay	Mm01258331_m1
Mouse Hamp TaqMan gene expression assay	Mm04231240_s1
Mouse Slc40a1 (Fpn) TaqMan gene expression assay	Mm00489837_m1

## Supplemental Figure

**Supplemental Figure 1. (A)** Treatment of HepG2 FPN-GFP cells with Dox reduced the level of intracellular ferritin heavy-chain (FTH1), consistent with increased iron export in cells expressing FPN-GFP. GAPDH was used as a loading control. **(B)** Images of untreated HepG2 cells, and cells treated with doxycycline (Dox; 2  $\mu$ g/ml) alone, with Dox followed by BMP6 (10 ng/ml) for 18 h and with Dox followed by chloroquine (100  $\mu$ M) and BMP6 (10 ng/ml) for 18h are shown.

**Supplemental Figure 2. (A)** The ratio of FPN levels in cells treated with Dox in the presence and absence of BMP6 was determined. The FPN protein ratio (Dox treatment/Dox+BMP6 treatment) was lower in siUBA6-treated cells compared to siControl- or siUBA1-treated cells (\*\*=P<0.01, One-Way ANOVA; N=3). **(B)** UBA6 was successfully depleted using siUBA6, despite the presence of exogenous BMP6, as determined by qPCR (mRNA expression relative to control; \*=P<0.05; Student's t-test). **(C)** HepG2-FPN-GFP cells were transfected with siControl-, siUBA6-, siNDFIP1 or siARIH1 and incubated in the presence of hepcidin (4 ng/ml for 18 h). siRNA directed against UBA6 and NDFIP1, but not ARIH1, prevented hepcidin-induced degradation of the FPN-GFP fusion protein, as determined by immunoblot. GAPDH was used as a loading control.

**Supplemental Figure 3. (A)** Cells were transfected with siControl, siSMAD4, siUBE2E2, siUBE2J2, or siUBE2R2 and were treated with Dox or Dox followed by BMP6 (10 ng/ml for 18 h), as indicated. White bar indicates 100  $\mu$ m. **(B)** The levels of FPN-GFP in cells treated with Dox and siRNAs directed against UBE2E2, UBE2J2 or UBE2R2 in the presence of BMP6 (10ng/ml for 18h) are shown. In lane 1, HepG2 cells were not treated with Dox (negative control). siRNA directed against *HAMP* was used as a positive control for inhibition of BMP6-mediated degradation of FPN-GFP. GAPDH was used as a loading control **(C)** NDFIP1 was successfully depleted using siNDFIP1 despite the presence of exogenous BMP6, as determined by qPCR (mRNA expression relative to control; \*\*=P<0.01; Student's t-test). **(D)** The ratio of FPN levels in the

presence and absence of BMP6 (FPN protein ratio of Dox treatment/Dox+BMP6 treatment) was determined. The ratio is lower in siNDFIP1- treated cell compared to siControl- and siNDFIP2-treated cells (\*=P<0.05, \*\*=P<0.01, One-Way ANOVA; N=4).

**Supplemental Figure 4. (A)** Levels of FPN-GFP in cells treated with Dox and siRNAs directed against different HECT E3 ligases (SMURF1, SMURF2, HECW1, HECW2, WWP1, WWP2, NEDD4, NEDD4-2, ITCH) in the presence (+) or absence (-) of BMP6 (10ng/ml for 18h). In lane 1, HepG2 cells were not treated with Dox (negative control). siRNA directed against *SMAD4* was used as a positive control for inhibition of BMP6-mediated degradation of FPN-GFP. GAPDH was used as a loading control. **(B)** Levels of FPN-GFP in cells treated with Dox and siRNAs directed against different HECT E3 ligases in pairwise combination. Cells were treated with BMP6 (10ng/ml) for 18h. siRNAs directed against HECT E3 ligases in pairwise combinations did not prevent the degradation of FPN-GFP. GAPDH was used as a loading control. **(C)** ARIH1 was successfully depleted using siARIH1, despite the presence of BMP6, as determined by qPCR (mRNA expression relative to control; \*\*=P<0.01; Student's t-test). **(D)** The ratio of FPN levels with and without BMP6 was lower in siARIH1-treated cells compared to siControl- and siARIH2- treated cells (\*=P<0.05, \*\*=P<0.01, One-Way ANOVA; N=4).

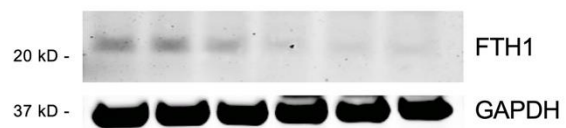
**Supplemental Figure 5. (A)** In AAV2/8-treated mice, the levels of hepatic ferroportin were positively correlated with serum iron (Pearson Correlation: R=0.6773; P=0.03). **(B)** The level of ferritin light chain (FTL) in the liver of AAV2/8-sh*Ndfip1* treated mice was increased compared to AAV2/8-sh*Control*-treated mice as determined by immunoblot. GAPDH was used as a loading control. **(C)** Densitometric analysis of immunoblot in (B) (\*\*=P<0.01, Student's t-test). **(D)** The mRNA expression of *TfR1* in the liver of AAV2/8-sh*Ndfip1*-treated animals was reduced compared to AAV2/8-sh*Control*-treated mice (\*\*=P<0.01, Student's t-test). **(E)** The level of splenic *Ndfip1* was similar in AAV2/8-sh*Control*- and AAV2/8-sh*Ndfip1*-treated animals, as determined by qPCR

## References

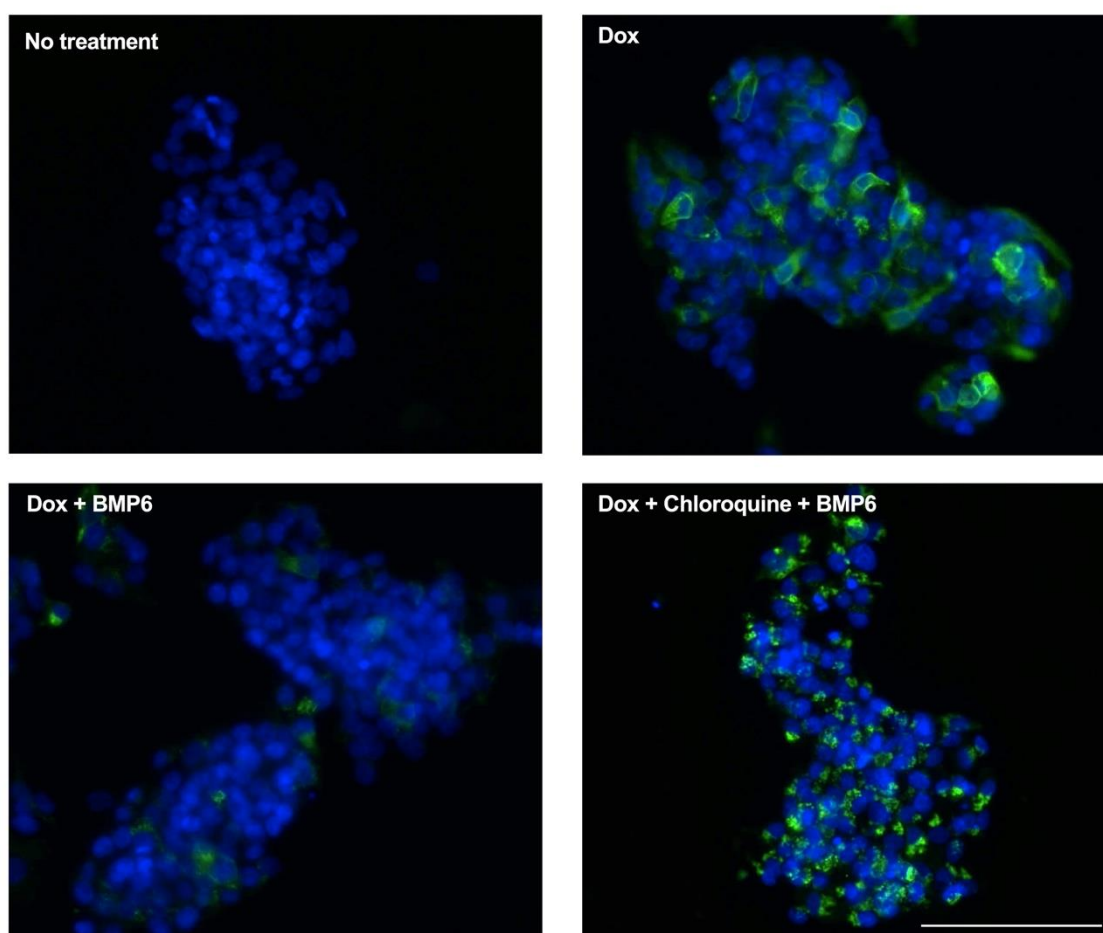
1. Canonne-Hergaux F, Donovan A, Delaby C, Wang H, Gros P. Comparative studies of duodenal and macrophage ferroportin proteins. *Am J Physiol Gastrointest Liver Physiol* 2006;290(1):G156-163.
2. Pfaffl MW. A new mathematical model for relative quantification in real-time RT-PCR. *Nucleic Acids Res* 2001;29(9):e45.

## Supplemental Figure 1

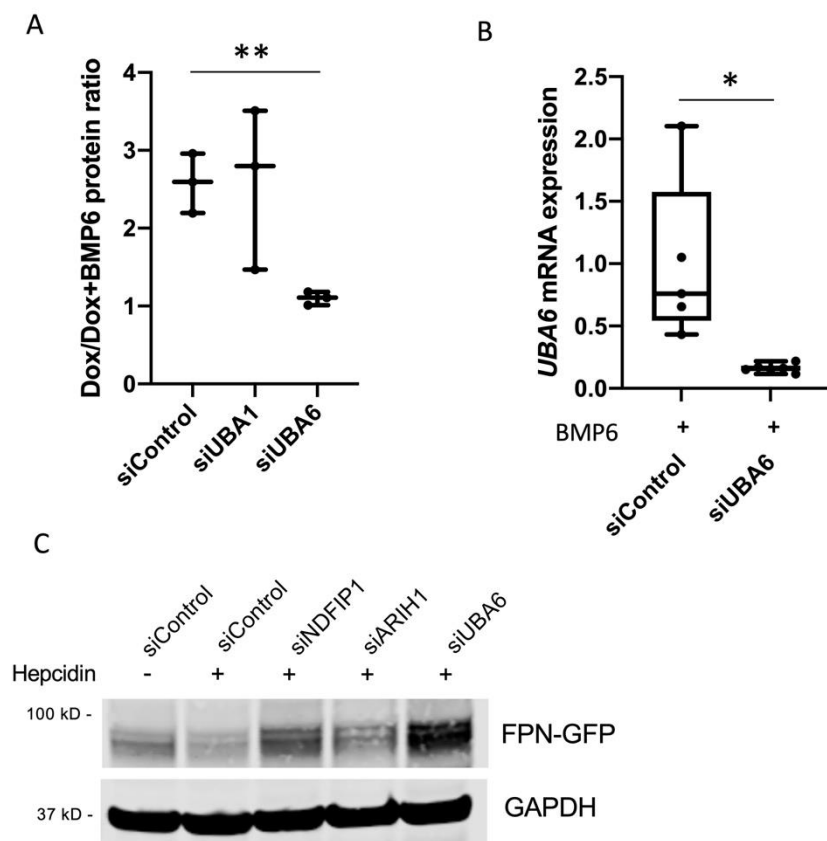
A



B

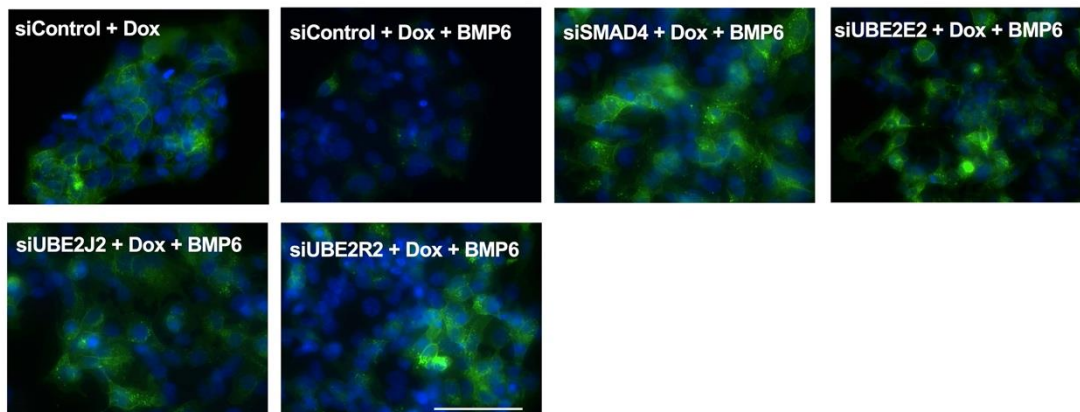


Supplemental Figure 2

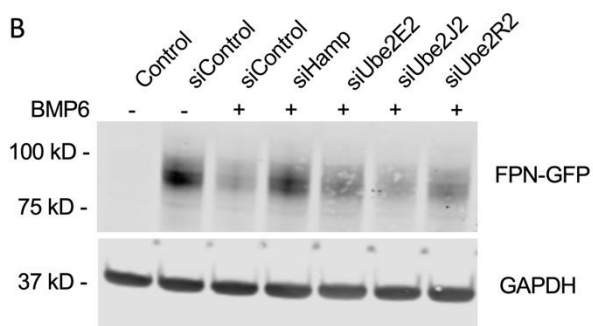


## Supplemental Figure 3

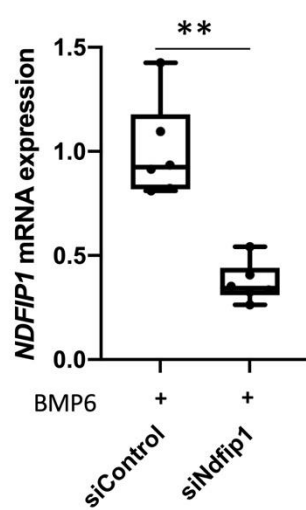
A



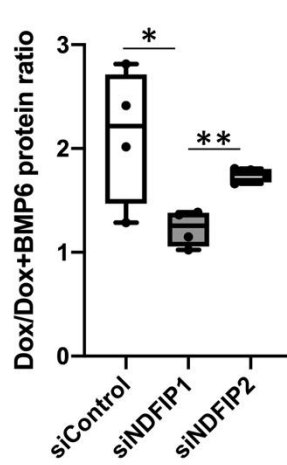
B



C

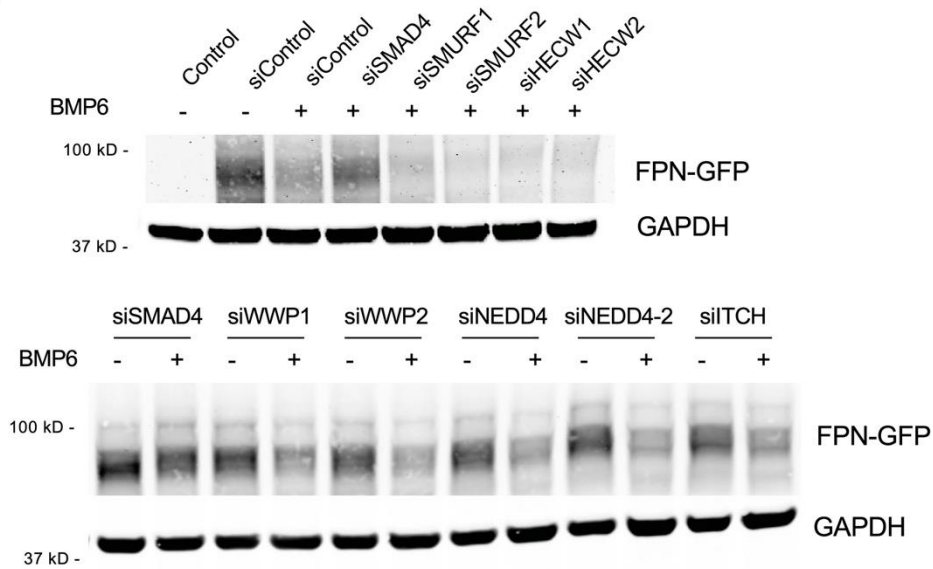


D

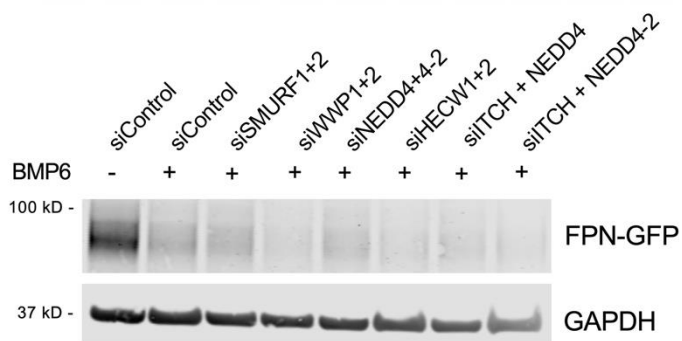


Supplemental Figure 4

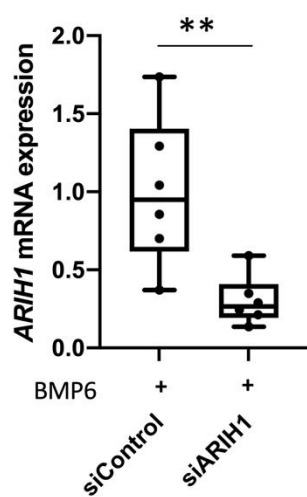
A



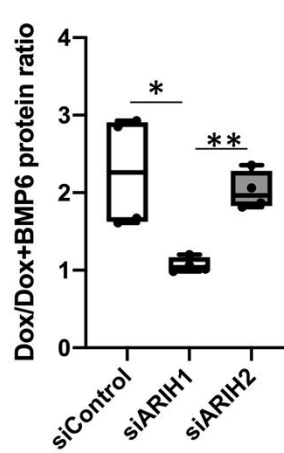
B



C



D



Supplemental Figure 5

